

Local ordering and charge transfer during room-temperature annealing of quenched tetragonal $\text{YBa}_2\text{Cu}_3\text{O}_{6.25}$

H. Shaked,* J. D. Jorgensen, B. A. Hunter, R. L. Hitterman, A. P. Paulikas, and B. W. Veal

*Materials Science Division and Science and Technology Center for Superconductivity,
Argonne National Laboratory, Argonne, Illinois 60439*

(Received 7 July 1994)

Neutron powder diffraction was used to study the crystallographic structure of a quenched tetragonal sample of $\text{YBa}_2\text{Cu}_3\text{O}_{6.25}$ during room-temperature annealing. It is found that the lattice parameters decrease with anneal time. The time dependence of the two lattice parameters is characterized by a single relaxation time ~ 760 min. Similar relaxation times were recently found for the electrical resistances R_{ab} , R_c , in tetragonal single crystals of $\text{YBa}_2\text{Cu}_3\text{O}_{6.25}$. These results are interpreted in terms of local ordering of the oxygen ions in the basal CuO_x plane, leading to a charge transfer between the CuO_x and CuO_2 planes. It is the same effect that leads to the rise in T_c observed earlier in orthorhombic $\text{YBa}_2\text{Cu}_3\text{O}_{6+x}$ ($x > 0.35$). The mechanism of the local ordering and the concept of oxygen ions ordering in a structure with tetragonal symmetry are discussed.

I. INTRODUCTION

Samples of $\text{YBa}_2\text{Cu}_3\text{O}_{6+x}$ quenched from $\sim 510^\circ\text{C}$ show remarkable annealing effects at room temperature (RT). Quenched nonsuperconducting ($x \sim 0.38$) samples become superconducting and the T_c 's of quenched superconducting samples ($0.4 < x < 0.9$) increase during RT annealing.^{1,2} These changes are accompanied by structural changes, e.g., quenched tetragonal samples ($x \sim 0.38$) become orthorhombic, and quenched orthorhombic samples show an increase in orthorhombicity.^{1,2} The T_c rise and the structural changes show time dependencies with a common characteristic relaxation time.

This intriguing behavior is explained as follows.¹⁻⁴ At high temperature, the equilibrium phase of $\text{YBa}_2\text{Cu}_3\text{O}_{6+x}$ is tetragonal with the oxygen ions randomly distributed on the O(1) site in the basal CuO_x plane (Fig. 1, $a = b$). At low temperature, the equilibrium phase is orthorhombic⁵⁻⁸ ($x > 0.35$) with the oxygen ions ordered in chains along the b axis ($b > a$, Fig. 1). When quenched from high temperature to a low temperature, some disorder of the oxygen ions in the CuO_x plane is retained. At this point in time, local ordering (i.e., ordering of the oxygen ions to form chain fragments) proceeds through thermal diffusion of the oxygen ions. Indeed, characteristic relaxation times of 300 to 600 min found^{1,2} for the T_c rise and the structural changes are in agreement with thermal diffusion rates of the oxygen ions at RT.^{1,2,9} The net effect on the basal CuO_x plane as an isolated oxygen ion joins a chain fragment, is that a threefold Cu^{2+} ion is converted into a twofold Cu^{1+} ion. This conversion requires an electron which is taken from the CuO_2 planes, leaving behind one hole which provides doping for the CuO_2 planes.⁴ In a recent study of the optical reflectance of a quenched sample of $\text{YBa}_2\text{Cu}_3\text{O}_{6.5}$, a 14% increase in hole concentration was found¹⁰ during RT annealing. This increase showed a characteristic relaxation time of ~ 500 min. This result provides direct evidence of the role played by charge transfer in relation

to the rise observed in T_c during RT annealing of quenched samples. Experimental evidence for the existence of chain fragments is provided by electron diffraction.^{11,12} Theoretical support for the possible existence of chain fragments is given in several publications.^{5,7,8,13,14}

Previous studies of RT annealing effects were performed in the oxygen composition range $0.35 < x < 0.5$, where $\text{YBa}_2\text{Cu}_3\text{O}_{6+x}$ is orthorhombic, and oxygen ion ordering (in chains) is consistent with symmetry and is expected thermodynamically.^{5,7,8} Recently, a strong anneal-

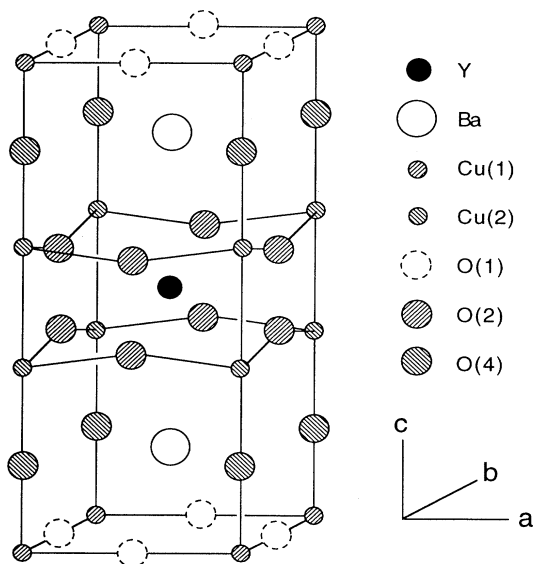


FIG. 1. A unit cell of the crystal structure of $\text{YBa}_2\text{Cu}_3\text{O}_{6+x}$. At high temperature, $a = b$, and the oxygen ions are uniformly distributed over the O(1) sites (dashed open circles). At RT, the oxygen forms O-Cu-O . . . chain fragments along b with most of the O(1) sites between the chains (i.e., on the a axis) being vacant.

ing effect of the electrical resistance was found¹⁵ in quenched single crystals of $\text{YBa}_2\text{Cu}_3\text{O}_{6.26}$ with tetragonal symmetry. During low-temperature anneals ($30 < T_{\text{anneal}} < 150^\circ\text{C}$), the in-plane resistance R_{ab} and the out-of-plane resistance R_c exhibited a long relaxation time with a RT value of ~ 800 min. In addition, R_{ab} also exhibited a short relaxation time with a RT value of ~ 30 min.

The crystallographic changes accompanying these effects in tetragonal $\text{YBa}_2\text{Cu}_3\text{O}_{6.26}$ are studied in the present work using neutron powder diffraction. We discuss the results in terms of the oxygen ordering and charge transfer model.^{1,2,4,5,7} We explore the RT annealing effects on the structure of $\text{YBa}_2\text{Cu}_3\text{O}_{6.26}$ which has a tetragonal symmetry where, strictly speaking, chains are not allowed.

II. EXPERIMENT

Sintered polycrystalline ceramic $\text{YBa}_2\text{Cu}_3\text{O}_{6+x}$ was prepared from powders of Y_2O_3 , BaCO_3 , and CuO using conventional techniques (e.g., see Ref. 2). The sintered bulk sample was then broken into coarse pieces. The fine particles were screened out leaving 10 g of material, consisting of 2–4 mm chunks. The oxygen stoichiometry of the 10 g sample was then fixed by heat treating the sam-

ple for 160 h at 510°C in flowing atmosphere of 0.01% O_2 in N_2 . The oxygen pressure was continuously monitored with an Ametek zirconia-cell oxygen pressure indicator. After the heat treatment, the sample was quenched to liquid nitrogen. This process produces a $\text{YBa}_2\text{Cu}_3\text{O}_{6+x}$ sample with a nominal oxygen stoichiometry $6+x \approx 6.25$. This stoichiometry determination is based on measurements using idometric titration.²

The sample, consisting of 2–4 mm chunks was kept in liquid nitrogen following its quench. The sample was transferred, in a bag filled with helium gas, while still cold, into a sealed vanadium can, and immediately mounted in the Special Environment Powder Diffractometer (SEPD) at Argonne's Intense Pulsed Neutron Source (IPNS).¹⁶ Data collection started about 5 min after the sample was removed from the liquid nitrogen. Since the SEPD is a time-of-flight diffractometer, the entire diffraction pattern is collected simultaneously. Sequential data sets were collected with collecting times as follows: six sets of 5 min, six sets of 10 min, six sets of 20 min, six sets of 40 min, twenty sets of 1 h, ten sets of 2 h, and five sets of 4 h. In total, 59 data sets were collected, without moving the sample, for a total elapsed time of 66 h.

The IPNS program for Rietveld analysis of the time-

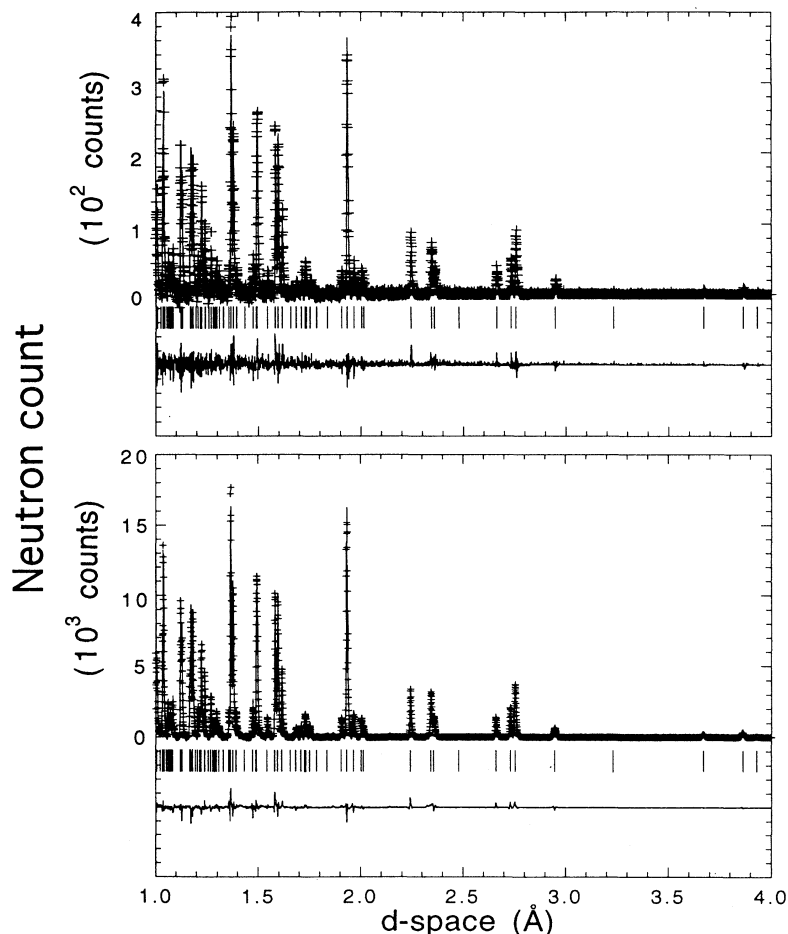


FIG. 2. Portion of the Rietveld refinement profile of the $\text{YBa}_2\text{Cu}_3\text{O}_{6.25}$ polycrystalline sample: 5 min collection time at ~ 30 min elapsed time (top), and 4 h collection time at ~ 60 h elapsed time (bottom). The plus symbols (+) represent the raw time-of-flight neutron-powder-diffraction data. The solid line represents the calculated profile. Tick marks represent the calculated positions of the allowed Bragg reflections. The background was fit as a part of the refinement, but has been subtracted prior to plotting. A difference curve (observed minus calculated) is plotted at the bottom.

of-flight neutron-diffraction data¹⁷ was used to refine the structural parameters. The Rietveld analyses were done in the tetragonal $P4/mmm$ space group (No. 123) (Ref. 18) and included 948 Bragg reflections, over the range of d spacings from 0.4 to 4.0 Å. Scattering amplitudes used¹⁹ were (in units of 10^{-12} cm) 0.775, 0.525, 0.7718, and 0.5805 for Y, Ba, Cu, and O, respectively. The refined parameters included the lattice parameters, all variable atom positions, isotropic thermal parameters for all atoms, and an isotropic linewidth ($\sigma 1$). The fractional occupancy of the O(1) site was refined in a preliminary analysis (of the 59 data sets) which yielded a mean value of 0.12 ± 0.01 (0.01 is the standard deviation for the distribution of the occupancies refined for the 59 data sets). This result corresponds to $x = 0.24$ (0.02) in good agreement with the nominal composition $\text{YBa}_2\text{Cu}_3\text{O}_{6.25}$. In the final analysis the fractional occupancy of the O(1) site was fixed at 0.12. The refinements gave good fits with low R values and small standard deviations for all the data. For example, $R_{wp}/R_{exp} = 15.6\%/15.8\%$ for the first 5 min data sets, $R_{wp}/R_{exp} = 8.2\%/6.2\%$ for the 40 min data sets, and $R_{wp}/R_{exp} = 5.8\%/2.8\%$ for the 4 h data sets. (R values are defined in Ref. 17.) Typical Rietveld profiles for the 5 min data set collected at ~ 30 min elapsed time, and for the 4 h data set at ~ 58 h elapsed time (=time from the start of data collection) are shown in Fig. 2.

The time dependencies of the refined lattice parameters a and c and the ratio $c/(3 \times a)$ are shown in Fig. 3. The lattice parameters a and c go through a maximum at about 30 min of elapsed time. It is conjectured that this effect is due to sample warm up to RT, since the sample was still cold when mounted in the SEPD. To test this conjecture, we estimate the sample temperature immediately after mounting (i.e., during collection of the first data set). The published²⁰ values of RT thermal expansion coefficients of $\text{YBa}_2\text{Cu}_3\text{O}_7$ are $\alpha_a = 10.0 \times 10^{-6} \text{ K}^{-1}$ and $\alpha_c = 18.5 \times 10^{-6} \text{ K}^{-1}$. The observed initial lattice parameter depressions (relative to the zero time intercept of the exponential fit, solid line in Fig. 3) are $\Delta a \approx 4 \times 10^{-4} \text{ Å}$ and $\Delta c \approx 2 \times 10^{-3} \text{ Å}$. Substituting these values into $\Delta T \approx \Delta l / (l \times \alpha_l)$ ($l = a, c$), two independent estimates of the sample temperature depression (relative to RT) are obtained. The two estimates both yield $\Delta T \approx 10 \text{ K}$, a reasonable temperature differential, since the vanadium can felt cold to the touch, but did not accumulate frost when mounted in the SEPD.

A simple exponential decay fitted to the decrease of the lattice parameters a and c with elapsed time yielded a relaxation time of 760 (100) min (solid lines, Fig. 3), in excellent agreement with the long relaxations (~ 800 min) found for R_{ab} and R_c at RT.¹⁵ Unfortunately, it is not possible to tell if fast lattice relaxation [40 min, observed for R_{ab} (Ref. 15)] exists, because of the changing sample temperature within this time range (Fig. 3).

Small, but systematic variations with elapsed time are observed (Fig. 4) in the Cu(2)-Cu(2) (i.e., inter- CuO_2 plane) distance, the Cu(2)-O(4) bond length, and the Ba- CuO_x plane distance (Fig. 1). It is not possible to determine the relaxation time from these data. We have therefore used a simple exponential to fit this data with the re-

laxation time constrained to the value obtained for the variation of the lattice parameters (Fig. 3). In this analysis, where the amplitude was the only variable, we have obtained small but statistically significant trends (Fig. 4), which are meaningful in terms of the charge transfer model (*vide infra*). The isotropic temperature factors and the linewidth ($\sigma 1$) do not show (within experimental uncertainty) any systematic variation with elapsed time.

III. DISCUSSION OF RESULTS

The lattice parameters (present work, Fig. 3) and the resistances¹⁵ R_{ab} and R_c relax with a common characteristic time. This result is consistent with the model

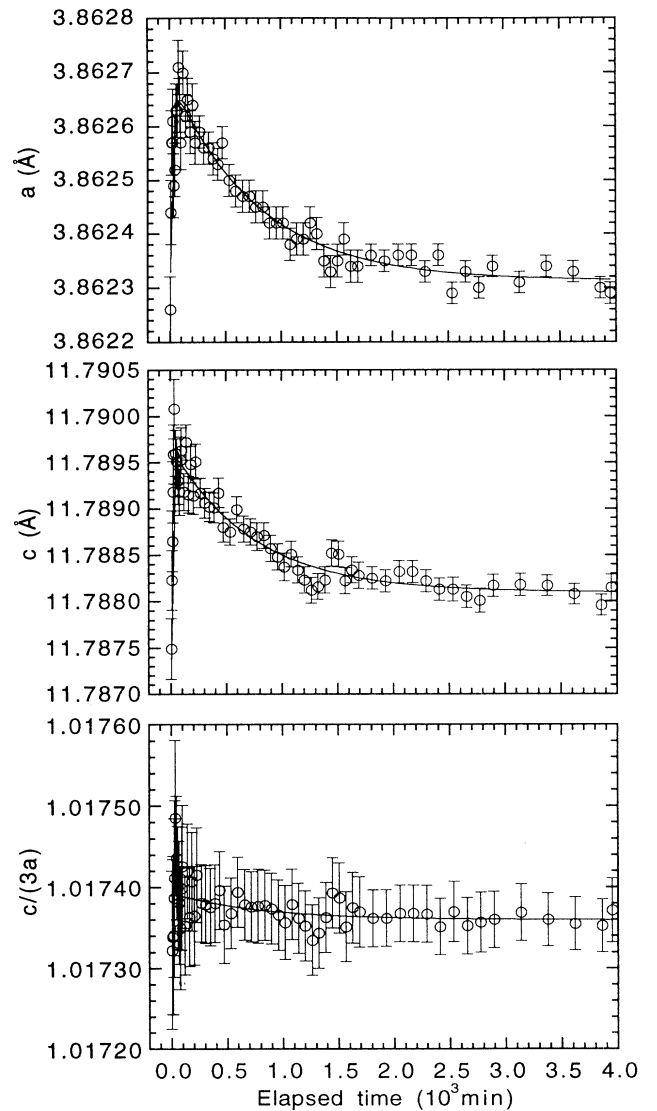


FIG. 3. Lattice parameters a and c (obtained from the Rietveld refinement of the neutron-powder-diffraction data), and $c/(a \times 3)$ vs elapsed time at RT for the quenched $\text{YBa}_2\text{Cu}_3\text{O}_{6.25}$ sample. The solid lines represent the best fit of a simple exponential decay [relaxation time = 760 (100) min]. For the first six points, the sample is still warming up toward RT.

proposed previously¹⁻⁴ of charge transfer resulting from oxygen ordering in samples with orthorhombic symmetry. The neutron-diffraction data of the present work, yielded a structure with a tetragonal lattice and an *average* oxygen occupancy of the O(1) site of 0.24. With such a low occupancy, less than $\frac{1}{8}$ of the O(1) site is occupied (Fig. 1). At high temperature (and in the as quenched samples) isolated oxygen ions are expected to be randomly distributed over the O(1) site [Fig. 5(a)]. At RT isolated oxygen ions migrate by thermal diffusion (*vide infra*) and form chain fragments. To preserve the overall tetragonal symmetry, the chain fragments must be equally distributed along the *a* and *b* axes [Fig. 5(b)]. In such a

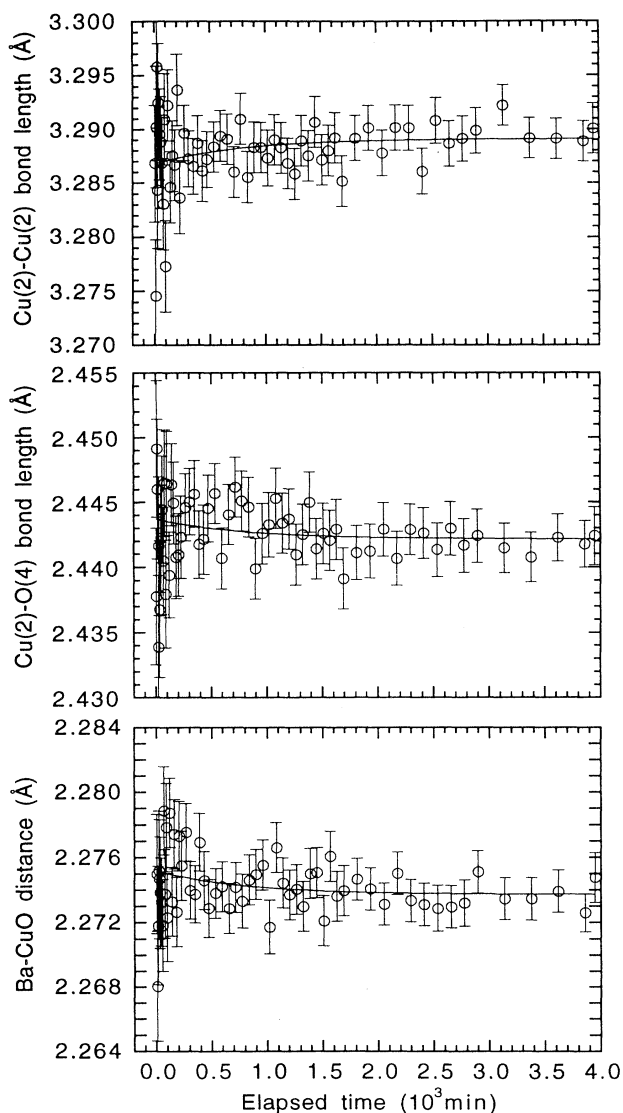


FIG. 4. Cu(2)-O(2) distance, Cu(2)-O(4) bond length, and Ba-CuO_x distance (obtained from the Rietveld refinement of the neutron-powder-diffraction data) vs elapsed time for the quenched YBa₂Cu₃O_{6.25} sample. The solid lines represent the best fit of a simple exponential with a relaxation time fixed at the value obtained in the fit to the lattice parameters (760 min).

structure, the local symmetry in a very small region around the chain fragment is lower than tetragonal. The large regions probed by neutron diffraction represent the average tetragonal structure where this local reduction in symmetry is averaged out. The reduction in symmetry was observed²¹ in tetragonal TmBa₂Cu₃O_{6+x} using inelastic neutron scattering by crystalline electric field (CEF) levels of the Tm ion (this is a single-ion effect, hence an extremely local probe). Structures of this type, arranged in small tweed domains, were also obtained by numerical simulations.²²

When an oxygen atom is added to the basal CuO_x plane and goes into an isolated position on the O(1) site (i.e., a position where it does not share its nearest Cu atoms with other oxygen atoms), it converts to an O²⁻ ion by removing one electron from each of its two Cu¹⁺ nearest neighbors, thereby raising their oxidation state from Cu¹⁺ to Cu²⁺. This process (unlike chain forming, *vide supra*) does not require a transfer of electrons from (or to) the CuO₂ planes. In the framework of this model⁴ all structures with isolated oxygen ions in the basal CuO_x plane do not support charge transfer. Hence, in this class of structures, the basal CuO_x plane does not serve as a charge reservoir. Various ordered structures that were previously proposed, namely, the alternating half-

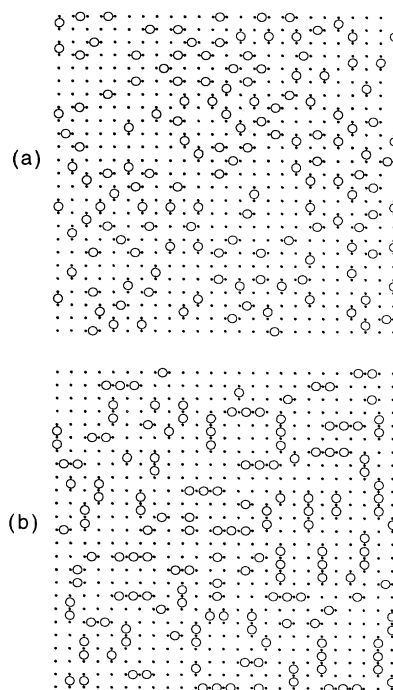


Fig. 5. Representation of the proposed local structure of the basal CuO_{0.25} plane. Oxygen ions are represented by open circles, and copper ions by black dots. (a) At 510°C: oxygen ions are randomly distributed on the O(1) site, with a constraint excluding two or more oxygen ions sharing a Cu ion. (b) At RT: Local ordering of the oxygen ions; oxygen ions form chain fragments.

filled-quarter-filled chains sequence,²³ [Fig. 6(a)] or the “herring-bone-type” structure,²⁴ [Fig. 6(b)] belong to this class. In these structures, there are no Cu ions with valence greater than $2+$, hence cuprates of this class are expected to be insulating.

We suggest that the oxygen ion ordering takes place via thermal diffusion for the following reasons. (i) The relaxation time corresponding to thermal diffusion of oxygen ions in the basal CuO_x plane can be estimated from the relation $t = \langle s \rangle^2 / (4D)$, where $\langle s \rangle$ is the diffusion length and D is the thermal diffusion coefficient. Using 4 \AA (\sim unit-cell edge) for $\langle s \rangle$ and $8 \times 10^{-21} \text{ cm}^2/\text{sec}$ for D ,⁹ we obtain $t = 820 \text{ min}$ in good agreement with the relaxation time observed in the present work. (ii) As the concentration of oxygen ions on O(1) is increased, the relaxation time decreases from $\sim 760 \text{ min}$ found in the present work for $x = 0.26$ to $\sim 400\text{--}500 \text{ min}$ found for $x = 0.41$.^{1,2} Assuming thermal diffusion, this is explained as follows: For lower concentrations, oxygen has to migrate a longer distance to join a chain fragment, hence, larger $\langle s \rangle$ and therefore larger t . (iii). As the anneal temperature is increased above RT, the relaxation time decreases.¹⁵ At $\sim 150^\circ\text{C}$ it becomes too short to be measured.^{1,15} This behavior is consistent with thermal diffusion where D undergoes a fivefold increase as temperature is increased from RT to 150°C ,⁹ and the relaxation time will correspondingly decrease to $\sim 1 \text{ sec}$.

The lattice parameter a shows a decrease during the RT anneal (Fig. 3). This decrease is due to shortening of the Cu(2)-O(2) bond. Since Cu^{3+} is smaller than Cu^{2+} ,²⁵

this shortening is consistent with our model of charge transfer [i.e., increased oxidation of the Cu ions on the Cu(2) site]. The bond valence sum (BVS) (Ref. 26) on the Cu(2) site calculated for the refined position parameters for our data (not corrected for strains) was found to increase from 2.032 to 2.035 during the RT anneal, while a decreased from 3.8627 to 3.8623 \AA . This yields a hole coefficient for a , $da/dn = -0.0004/0.003 = -0.13 \text{ \AA}/\text{hole}/\text{Cu}(2)$. This result is in good agreement with the expected value of $-0.056/0.4 = -0.14 \text{ \AA}/\text{hole}/\text{Cu}(2)$ (calculated from Table II, Ref. 26). The Cu(2)-O(4) bond length and the Ba ion-CuO_x plane distance decrease, and the Cu(2)-Cu(2) interplane distance increases during the RT anneal (Fig. 4). Changes of the same signs were observed⁶ as oxygen was added to $\text{YBa}_2\text{Cu}_3\text{O}_{6+x}$ (x is increased). These changes are consistent with what is expected in a simple model of electrostatic forces when holes (positive charge) are transferred from the CuO_x plane to the CuO_2 planes.

The derivative dT_c/dn [where n is the number of holes in the CuO_2 plane per Cu(2) ion] estimated from ellipsometric measurements of $\text{YBa}_2\text{Cu}_3\text{O}_{6.35}$ is equal to 543 K/hole/Cu(2).¹⁰ Using this estimate, the charge transfer Δn [i.e., the increase in number of holes per Cu(2), during the RT anneal] is estimated (Table I) from the measured changes in a , Δa , and/or T_c , ΔT_c for various values of x (Refs. 1, 2, and the present work). The estimated Δn versus x shows a remarkable maximum at $x \approx 0.35$ (Fig. 7). Although, this graph represents a crude (the quenching conditions are not identical in the different samples) estimate of Δn (see Table I), its qualitative features (i.e., $\Delta n \rightarrow 0$ as $x \rightarrow 0$ and 1) are in agreement with calculations using a chemical valence model,⁴ and are probably valid. It is interesting that Δn reaches its maximum at $x \sim 0.35$, at the same composition where $\text{YBa}_2\text{Cu}_3\text{O}_{6+x}$ undergoes a tetragonal to orthorhombic phase transition and becomes superconducting.

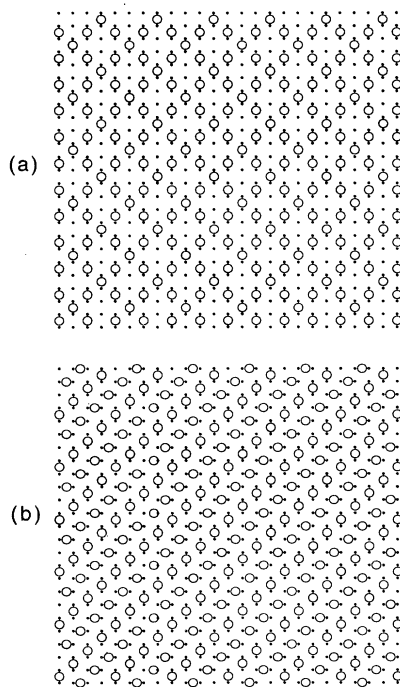


FIG. 6. Ordered structures of the basal CuO_x plane. Oxygen ions are represented by open circles, and copper ions by black dots. (a) $x = 0.375$, half-filled-quarter-filled chains sequence (Ref. 23); (b) $x = 0.5$, “herring-bone-type” structure (Ref. 24).

TABLE I. Changes that take place during RT anneal of $\text{YBa}_2\text{Cu}_3\text{O}_{6+x}$: measured change, Δa , in lattice parameter, a ; measured change, ΔT_c , in T_c ; calculated change, Δn , in the number of holes per Cu(2), n ; $\Delta n = \Delta a / (da/dn)$ and/or $= \Delta T_c / (dT_c/dn)$. The following values for the derivatives were used: $dT_c/dn = 543 \text{ K}/\text{hole}/\text{Cu}(2)$ (from the ellipsometric measurements reported in Ref. 10), and $da/dn = (\Delta a / \Delta T_c) \times (dT_c/dn) = (-0.0019/11) \times 543 = 0.094 \text{ \AA}/\text{hole}/\text{Cu}(2)$ (from Refs. 1 and 2).

x	Δa (10^{-4} \AA)	ΔT_c (K)	Δn [$10^{-3} \text{ holes}/\text{Cu}(2)$]
0.26	-4 ^a		4
0.30	-17 ^b		18
0.41	-19 ^c	11 ^b	20
0.45		8 ^b	15
0.50		6 ^b	11
0.60		2 ^b	4

^aPresent work.

^bReference 1.

^cReference 2.

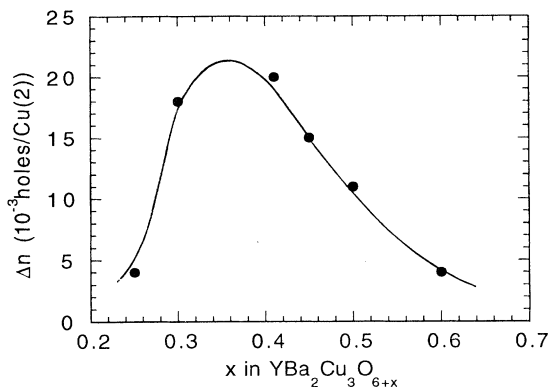


FIG. 7. The increase in number of holes in the CuO_2 planes per $\text{Cu}(2)$ ion, Δn , during RT annealing vs x in $\text{YBa}_2\text{Cu}_3\text{O}_{6+x}$ (see Table I). The solid line is a guide to the eye.

IV. CONCLUSION

RT annealing of quenched samples of $\text{YBa}_2\text{Cu}_3\text{O}_{6+x}$ shows a relaxation of the electrical resistance,¹⁴ a decrease of lattice parameters, and (for $x > 0.35$) a rise in T_c . We conclude that these effects, which have a common relaxation time τ result from local ordering of the oxygen ions of the basal CuO_x plane into chain fragments. This ordering requires a transfer of electrons from the CuO_2 plane to the basal CuO_x plane. This

charge transfer dopes the CuO_2 plane with holes, and completely explains the three effects observed during the RT anneal.

The oxygen ordering (and therefore the charge transfer) is controlled by thermal diffusion. Hence, the relaxation time for these effects scales with the diffusion length, and with the inverse of the thermal diffusion coefficient and, thus, decreases with concentration of oxygen ions in the basal CuO_x planes and with temperature.

For $x < 0.38$, the symmetry of the average structure (i.e., as determined by diffraction experiments) is tetragonal. The formation of chain fragments (local ordering) reduces the local symmetry, but since the chain fragments are equally distributed along the a and b axes, the average tetragonal symmetry is preserved. For $x > 0.38$, all the chain fragments are aligned along a single axial direction and the average symmetry is reduced to orthorhombic.

ACKNOWLEDGMENTS

This work was supported by U.S. Department of Energy, Division of Basic Energy Sciences—Material Sciences, under Contract No. W-31-109-ENG-38 (J.D.J., R.L.H., A.P.P., B.W.V.), the National Science Foundation, Science and Technology Center for Superconductivity under Grant. No. DMR 91-20000 (H.S., B.A.H.), and the Nuclear Research Center—Negev and Ben-Gurion University in the Negev (H.S.).

*Permanent address: Department of Physics, Nuclear Research Center—Negev, P.O.B. 9001, Beer Sheva, Israel 84190 and Department of Physics, Ben-Gurion University of the Negev, P.O.B. 653, Beer Sheva, Israel 84105.

¹B. W. Veal, A. P. Paulikas, H. You, H. Shi, Y. Fang, and J. W. Downey, *Phys. Rev. B* **42**, 6305 (1990).

²J. D. Jorgensen, S. Pei, P. Lightfoot, H. Shi, A. P. Paulikas, and B. W. Veal, *Physica C* **167**, 571 (1990).

³A. N. Lavrov, *Physica C* **216**, 36 (1993).

⁴B. W. Veal and A. P. Paulikas, *Physica C* **184**, 321 (1991).

⁵H. F. Poulsen, N. H. Andersen, J. V. Andersen, H. Bohr, and O. G. Mouritsen, *Nature* **349**, 594 (1991).

⁶R. J. Cava, A. W. Hewat, E. A. Hewat, B. Batlogg, M. Marezio, K. M. Rabe, J. J. Krajewski, W. F. Peak, Jr., and L. W. Rupp, Jr., *Physica C* **165**, 419 (1990).

⁷G. Ceder, R. McCormak, and D. de Fontaine, *Phys. Rev. B* **44**, 2377 (1990).

⁸J. L. Moran-Lopez and J. M. Sanchez, *Physica C* **210**, 401 (1993).

⁹S. J. Rothman, J. L. Routbort, U. Welp, and J. E. Baker, *Phys. Rev. B* **44**, 2326 (1991).

¹⁰J. Kircher, M. Cardona, A. Zibold, K. Widder, and H. P. Geserich, *Phys. Rev. B* **48**, 9684 (1993).

¹¹H. Horiuchi, *Jpn. J. Appl. Phys.* **31**, L1335 (1992).

¹²S. Yang, H. Claus, B. W. Veal, R. Wheeler, A. P. Paulikas, and J. W. Downey, *Physica C* **193**, 243 (1992).

¹³V. M. Matic, *Physica C* **211**, 217 (1993).

¹⁴A. Renault, J. K. Burdett, and Jean-Paul Pouget, *J. Solid*

State Chem. **71**, 587 (1987).

¹⁵A. P. Paulikas and B. W. Veal (unpublished).

¹⁶J. D. Jorgensen, J. Faber, Jr., J. M. Carpenter, R. K. Crawford, J. R. Haumann, R. L. Hitterman, R. Kleb, G. E. Ostrowski, F. J. Rotella, and T. G. Worlton, *J. Appl. Crystallogr.* **22**, 321 (1989).

¹⁷F. J. Rotella, Users Manual for Rietveld Analysis of Time of Flight Neutron Diffraction Data at IPNS, Argonne National Laboratory—IPNS report, 1988 (unpublished); R. B. VonDreele, J. D. Jorgensen, and C. G. Windsor, *J. Appl. Crystallogr.* **15**, 581 (1982).

¹⁸*International Tables for Crystallography, Volume A, Space-Group Symmetry*, edited by T. Hahn (Reidel, Dordrecht, 1987), p. 420.

¹⁹*International Tables for Crystallography, Volume C, Mathematical, Physical and Chemical Tables*, edited by A. J. C. Wilson (Reidel, Dordrecht, 1983), p. 384.

²⁰C. Meingast, O. Kraut, T. Wolf, H. Wuhl, A. Erb, and G. Muller-Vogt, *Phys. Rev. Lett.* **67**, 1634 (1991).

²¹B. A. Hunter and R. Osborn (unpublished).

²²S. Semenovskaya and A. G. Khachatryan, *Phys. Rev. B* **46**, 6511 (1992).

²³R. Sonntag, D. Hohlwein, T. Bruckel, and G. Collin, *Phys. Rev. Lett.* **66**, 1497 (1991).

²⁴Th. Zeiske, D. Hohlwein, R. Sontag, F. Kubanek, and G. Collin, *Z. Phys. B* **86**, 11 (1992).

²⁵R. D. Shannon, *Acta Crystallogr. A* **32**, 751 (1976).

²⁶I. D. Brown, *J. Solid State Chem.* **90**, 155 (1991).